NANO LETTERS

2008
Vol. 8, No. 8
2328-2335

Rotating Fullerene Chains in Carbon Nanopeapods

Jamie H. Warner,*,† Yasuhiro Ito,† Mujtaba Zaka,† Ling Ge,† Takao Akachi,‡ Haruya Okimoto,‡ Kyriakos Porfyrakis,† Andrew A. R. Watt,† Hisanori Shinohara,‡ and G. Andrew D. Briggs†

Department of Materials, Quantum Information Processing Interdisciplinary Research Center, University of Oxford, Parks Rd, Oxford, OX1 3PH, United Kingdom, and Department of Chemistry and Institute for Advanced Research, Nagoya University, Furo-Cho, Chikusa-ku, Nagoya, 464-8602, Japan

Received April 23, 2008; Revised Manuscript Received June 6, 2008

ABSTRACT

The rotation of fullerene chains in SWNT peapods is studied using low-voltage high resolution transmission electron microscopy. Anisotropic fullerene chain structures (i.e., C_{300}) are formed in situ in carbon nanopeapods via electron beam induced coalescence of individual fullerenes (i.e., C_{60}). A low electron accelerating voltage of 80 kV is used to prevent damage to the SWNT. The large asymmetric C_{300} fullerene structure exhibits translational motion inside the SWNT and unique corkscrew like rotation motion. Another asymmetric fullerene chain containing mixed fullerene species is prepared by fusing smaller C_{60} fullerenes to a larger $Sc@C_{82}$ fullerene, and this also exhibits corkscrew rotational motion. Chains of $Sc_3C_2@C_{80}$ in SWNT peapods adopt a zigzag packing structure, and the entire zigzag chain rotates inside the SWNT to induce structural modifications to the SWNT diameter and cross-sectional shape of the SWNT. The expansion and contraction of the diameter of the SWNT is measured as 17%, demonstrating nanoactuation behavior in carbon nanopeapods.

Single-walled carbon nanotubes (SWNTs) are excellent materials for nanomechanical and nanoelectronic device applications.[1] Semiconducting nanotubes can be doped to control and modify their properties at the nanoscale.[2] While there exist several methods to introduce dopant species to SWNTs, one of the most interesting and unique methods is to insert the dopant species directly into the hollow interior.[3] This type of doping has been shown to modify both the electronic transport and the mechanical properties of the SWNTs.[4–6] Many different types of fullerenes and metallofullerenes, such as C_{60},[7] C_{70},[8] C_{82},[9] $La@C_{82}$,[10] $La_2@C_{80}$,[11] $Gd@C_{82}$,[12] $Sc_2@C_{84}$,[13] and $Ce@C_{82}$, can be inserted into SWNTs to form peapods.[14] The encapsulation of fullerenes in SWNTs leads to a net energy gain that gives rise to a capillary force.[15] Encapsulation energies for the formation of exothermic peapods are typically up to 1 eV.[15] The capillary force is predicted to be in the nanonewton region and to generate pressures within the peapod of the order of a GPa for C_{60}@SWNT peapods.[15] The large internal pressure compresses the fullerenes and results in smaller interfullerene spacings than in bulk crystals.[9]

The one-dimensional (1D) spatial confinement inside the SWNT can lead to modifications of the chemical reactivity and motional dynamics of encapsulated molecular species. $C_{60}O$ encapsulated in SWNT peapods reacts to form covalent polymer chains that are different than the bulk polymer form.[16] When carborane molecules with alkyl side chains are encapsulated in SWNTs, their translational and conformational motion is suppressed.[17] C_{60} functionalized with pyrrolidine in SWNT peapods rotates during transmission electron microscopy (TEM) observation, and the functional group stands facing toward the nanotube wall.[18] The dynamical behavior of individual retinal chromophores confined in SWNTs revealed the isomerization between cis and all-trans forms of retinal.[19]

Transmission electron microscopy is an excellent tool for imaging and characterizing peapod structures with subnanometer resolution. The interaction of the electron beam of the TEM with carbon nanomaterials is critically dependent upon the accelerating energy used.[20] A high energy electron impinging upon a peapod imparts a small amount of its incident energy to a carbon atom via electron−nucleus scattering and electron−electron scattering.[20] If the energy of the electron is larger than the threshold energy necessary for displacing or ejecting a carbon atom due to electron−nucleus scattering, then irreversible damage is induced.[21–23] The high energy of the electron beam can be intentionally used to modify the properties of carbon nanomaterials and can create entirely new structures.[24–26] For example, electron beam

* Corresponding author. E-mail: Jamie.warner@materials.ox.ac.uk.
† University of Oxford.
‡ Nagoya University.

10.1021/nl801149z CCC: $40.75
Published on Web 07/02/2008

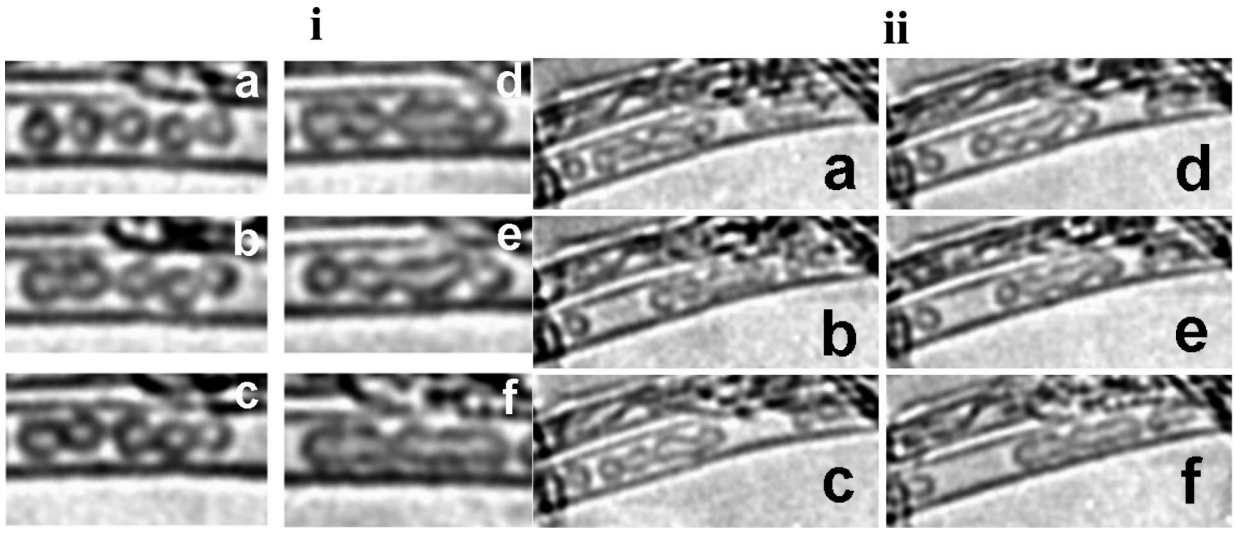

Figure 1. (i) Time series (a−f) of TEM images of 5 C_{60} fullerenes under constant electron beam irradiation, with 5 min between each image. (ii) Time-series (a−f) of TEM images showing the motion of the C_{300} structure formed via the coalescence of 5 C_{60} fullerenes, time between each frame is 10 s.

irradiation of carbon onions results in phase transformation to diamond.[26] The interaction of the electron beam with organic molecules encapsulated in the SWNT and carbon nanomaterials is often highly destructive.

The knock-on damage threshold for carbon nanomaterials is low (≤80 keV), and therefore damage can be easily induced in structures being examined with HRTEM.[27] Electron beam induced coalescence of C_{60} fullerenes in SWNT peapods has been previously reported using accelerating energy of 97−120 kV, well above the knock on damage threshold.[28] These observations have been theoretically modeled using molecular dynamics simulations, and the temperatures needed for this coalescence to occur have been predicted to be well over 1000 °C.[28] In these observations, it is difficult to separate the effect of heating and structural damage. Structural damage is evident in these studies by the distortion of the SWNT side walls.[28] Here, we show that novel fullerene structures can be formed by exposing fullerene chains in peapods to electron beam irradiation with an accelerating voltage of 80 kV, without damaging the SWNT host. By using electrons below the knock-on damage threshold, we were able to study the behavior of these structures over extended time periods and observe entirely new corkscrew like rotational dynamics in the peapod structures. These results provide an in-depth understanding of the unique behavior of different fullerene species in SWNT peapods.

Peapods were produced using the hot filling method.[29] Metallofullerenes were produced using the arc-discharge process and were purified using HPLC.[30] The SWNTs were purchased from Carbolex and were purified by annealing at 380 °C in air for 2 h and then refluxing in HCl acid for 8 h. A solution of fullerenes dispersed in CS_2 was dropped onto the SWNT powder, and the solvent was allowed to evaporate. The sample was then sealed in a quartz tube under vacuum and heated at 450 °C for 4 days to form peapods. The peapods were then dispersed in 1,2-dichloroethane using ultrasonication and were deposited onto lacey carbon grids for TEM analysis. TEM was performed using a JEOL 4000 operating at 80 kV with LaB_6 filament, with beam current density of 16−22 pA/cm^2. Peapods containing mixed species of C_{60} and Sc@C_{82} were formed by using a CS_2 solution with a C_{60}/Sc@C_{82} ratio of 40:1 to deposit onto the SWNTs. Peapods containing only one fullerene specie such as 100% C_{60}, Sc_3C_2@C_{80}, or Sc@C_{82} were also prepared.

Large fullerene structures were formed by fusing together several fullerenes that were initially packed in a 1D chain in the peapod. Fullerene coalescence was induced by long-term electron beam irradiation. Figure 1i shows a time series of TEM images of a section of a peapod containing five C_{60} fullerenes with the time between each image being 5 min. At the beginning of the irradiation, the fullerenes are distinguishable and separated, Figure 1ia. As time progresses, fullerenes 1 and 2 slowly fuse to form a dimer, while fullerenes 3−5 fuse to form a trimer, Figure 1ib,ic. After 30 min of constant electron beam irradiation the 5 fullerenes coalesce into one 5 nm long C_{300} structure, Figure 1if. It is important to note that, even after 30 min of constant electron beam irradiation, the sidewalls of the SWNT retained their integral structure and are straight and clean.

The as-formed C_{300} fullerene structure did not develop any attachement or bonding to the sidewalls of the SWNT. Figure 1ii shows a time series of TEM images taken after the C_{300} structure had been formed, with 10 s between each image. The entire C_{300} fullerene is free to move back and forth across the partially filled area of the peapod. This shows that the C_{300} structure is free from any SWNT attachment, similar to the case of pristine fullerenes (e.g., C_{60}) in peapods. This indicates that the fusing of the C_{60} is driven by a thermal process rather than through structural damage. As the C_{300} translates along the inside of the SWNT, it also rotates with an axis of rotation parallel to the axis of the SWNT.

Figure 2i determines the C_{300} orientation from the TEM images in Figure 1iic−f, with a schematic illustration to the right of each image. During this time series, the C_{300} changes its orientation by rotating inside the SWNT. The asymmetry

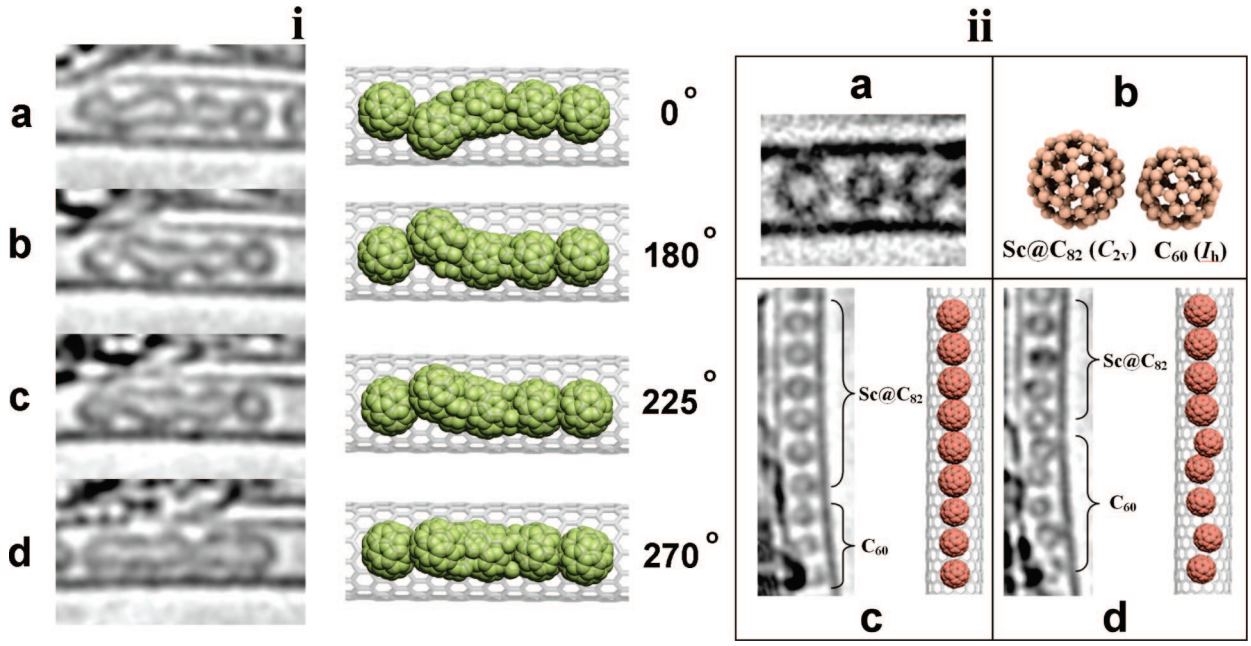

Figure 2. (i) Time series (a−d) of TEM images showing the rotation of the C_{300} structure inside the SWNT, with 10 s between each image. A schematic illustration is presented to the right of each image along with the relative orientation. (ii) (a) TEM image of two Sc@C_{82} separated by one C_{60} in the middle in a SWNT peapod. (b) Schematic structural representation of Sc@C_{82} (C_{2v}) and C_{60} (I_h) fullerenes. (c) TEM image showing a section of a mixed species peapod containing both Sc@C_{82} and C_{60} phases. (d) TEM image of a section of a peapod containing large C_{60} phase.

of the C_{300} structure allows the rotation to be monitored and the relative orientation to be determined. Figure 2i shows that long 5 nm structures such as the C_{300} structure can exhibit rotational motion inside SWNTs.

Large asymmetric fullerene structures could also be formed by fusing together C_{60} with Sc@C_{82} metallofullerenes in SWNT peapods containing a mixture of the two species. The overall size of Sc@C_{82} is between 13−28% larger in diameter than C_{60}, depending upon their relative orientation due to the nonspherical structure of the cages, and this enables their identification using HRTEM. Figure 2iia shows a HRTEM image of two Sc@C_{82} metallofullerenes separated by a C_{60} fullerene in a SWNT peapod. The larger size of the Sc@C_{82} is easily distinguished when compared with that of the C_{60}. The sizes of the two outer Sc@C_{82} metallofullerenes are ∼23% larger than the middle C_{60} fullerene. Figure 2iib shows the structural representation of Sc@C_{82} (C_{2v}) and C_{60} (I_h), illustrating the size difference between the two fullerenes. Several sections of peapods were examined to characterize the packing distribution of C_{60} and Sc@C_{82}. Figure 2iic shows a section of a peapod that enabled up to 11 fullerenes to be observed. This section was examined over several minutes, and the chain of fullerenes was observed to move along the inside of the SWNT like a train. At the beginning of the observation, the section contained at least 6 Sc@C_{82} situated together with regular 1D packing arrangement and no displacement in the radial direction of the SWNT. As time progressed, the six Sc@C_{82} moved upward and out of the viewing plane and were replaced by a section of C_{60} fullerenes, as shown in Figure 2iid. The C_{60} fullerenes adopted zigzag packing, with a significant degree of radial displacement due to their smaller size. As time further progressed, the phase of the material continued to change, proving that both C_{60} and Sc@C_{82} had been included into the one SWNT with mixed phases. The distribution of Sc@C_{82} and C_{60} seemed random; sometimes the Sc@C_{82} was well-separated by C_{60}, and other times there were chains of up to 10 C_{60} followed by chains of Sc@C_{82}.

A section of the peapod containing Sc@C_{82} well dispersed among the C_{60} was located using TEM. Figure 3ia shows two Sc@C_{82} separated by a C_{60} fullerene, schematically illustrated to the right. Figure 3ib is taken 10 s later and shows five C_{60} fullerenes arriving from the left-hand side. All of the fullerenes seem to be centered in the middle of the SWNT with minimal radial displacement. At this stage, the time of electron beam irradiation was ∼30 s and was insufficient to induce fusion. This structure was then irradiated with the electron beam for 5 min to induce fusion, shown in Figure 3ic. After this 5 min, the C_{60} attached to both sides of the Sc@C_{82} indicated with the asterisk and became displaced in the radial direction of the SWNT. Another TEM image was taken 10 s after this, Figure 3id, and shows the entire structure rotated 180°. The larger diameter of the Sc@C_{82} fits snugly into the SWNT and provides an axis of rotation along the SWNT axis. Another TEM image was taken 10 s after this, Figure 3ie, and shows the structure rotated 180° back to its original orientation.

The motion studied in Figure 3i is purely rotational with no translational motion along the axis of the SWNT. Further insights into the rotational dynamics are obtained by monitoring the rotational motion while the structure undergoes translational motion along the SWNT axis. Figure 3iia shows the initial position of the fused fullerene structure formed in the study presented in Figure 3i. Figure 3iib shows the fused fullerene structure moving away from the right-hand side. The Sc@C_{82} on the far right-hand side remains

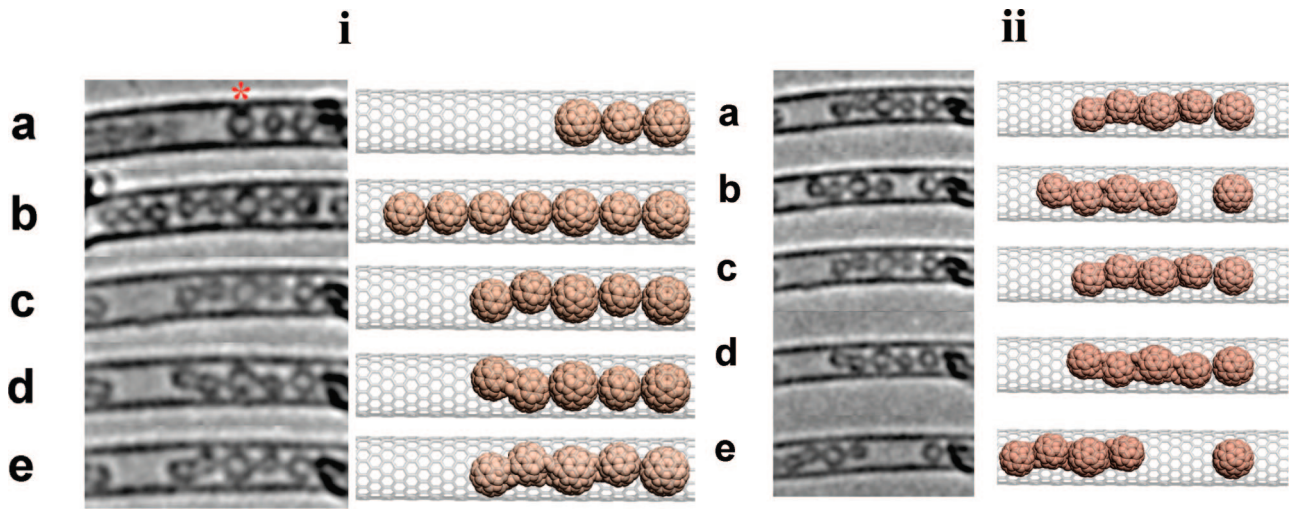

Figure 3. (i) (a) TEM image showing $Sc@C_{82}$ and C_{60} in SWNT peapod. (b) TEM image taken 10 s after that in part a, showing the arrival of five C_{60} from the left-hand side. (c) TEM image taken 5 min after that in part b, to induce the fusion of fullerenes. (d) TEM image taken 10 s after that in part c, showing rotation of 180°. (e) TEM image taken 10 s after that in part d, showing another 180° rotation. Two seconds are used for image acquisition in all cases. A schematic representation is presented to the right of each image. (ii). Time series (a−e) of TEM images showing the rotation during the translational motion of the large structure formed via fusing C_{60} to $Sc@C_{82}$ in SWNT peapod. Time between each image is 10 s, with 2 s for image acquisition. A schematic representation is presented to the right of each image.

in its location, and this indicates that the C_{60} was not attached to it and that the fullerene structure consists of three C_{60} and one $Sc@C_{82}$ attached to each other. As the four fullerenes move away, the structure rotates by nearly 180°. Figure 3iic shows the structure returning to its original location and also rotating a further 180° to return to its original orientation. Figure 3iid shows the structure rotating another 180° while remaining in the same location, similar to the observations in Figure 3i. Finally, in Figure 3iie, the structure moves a further distance to the left than previously observed in Figure 3iib. The far right-hand side $Sc@C_{82}$ again remains in its location, confirming that it is still not part of the fused structure. The structure has also rotated by 180° during its translational motion.

The TEM images presented in Figure 3 demonstrate that C_{60} can attach to $Sc@C_{82}$ to form chains of mixed fullerene species. As the C_{60} become fused to the $Sc@C_{82}$, they become displaced from the center of the SWNT in the radial direction. Figure 3iie shows that both of the two C_{60} attached to the $Sc@C_{82}$ lie close to the upper wall of the SWNT, and this indicates there may be some selective reactive sites between the two species that gives rise to this geometry. We found that when C_{60} fuses together they tend to form zigzag structures in SWNTs with diameters larger than 1.5 nm, with fullerenes alternating between touching the top and bottom walls of the SWNTs. These chains of fused mixed fullerene species are free to exhibit both translational and rotational motion inside the SWNT. In order to observe clear images of the fullerenes inside the SWNT, they must remain in a fixed orienation for the duration of the image acquisition. The fused chain then rapidly rotates to another orientation and remains stable in this orientation for sufficient time to acquire a clear TEM image. The large fullerene structures predominantly rotate by 180° intervals. The rotation of the chain is probably due to energy acquired during the electron beam irradiation, potentially from an impulse generated from the scattering of high-energy electrons.

We found that C_{60} fullerene chains were easier to fuse together than chains of metallofullerenes. Pyrimidalization and misalignment of π orbitals in curved graphene sheets results in strain of the C−C bond and gives rise to reactivity.[31,32] As the size of a fullerene cage or SWNT diameter decreases, the C−C bond strain increases, and this leads to enhanced chemical reactivity.[32] The smaller diameter of C_{60} compared with that of $Sc@C_{82}$ results in larger C−C bond strain and potentially higher reactivity. The charge transfer in metallofullerenes may also introduce other effects such as repulsive Coulomb forces and exchange interactions that may influence the interfullerene reactions. It is also important to note that the fullerenes do not fuse to the side walls of the SWNT and that fusion takes place between the two opposing convex surfaces of the fullerenes.

Peapods containing 100% metallofullerenes displayed different behavior under long-term electron beam irradiation at 80 kV than peapods containing C_{60}. In peapods containing pure $Sc_3C_2@C_{80}$, we observed the rotation of 10 nm long zigzag chains inside the SWNTs that resulted in the expansion and contraction of the SWNT diameter. The section of SWNT peapod contained one end that was pinched off and prevented the propagation of fullerenes beyond this point (Supporting Information, S1). Figure 4i presents a time series of TEM images from this $Sc_3C_2@C_{80}$ metallofullerene SWNT peapod, with the pinched section to the right-hand side. Each image is taken with 2 s exposure and 10 s between each image. In Figure 4ia, the peapod has regular 1D packing of the $Sc_3C_2@C_{80}$ in the SWNT. As time progresses, the diameter of the SWNT begins to expand (Figure 4ic) then contract back to the original diameter (Figure 4id), followed by a larger expansion (Figure 4if) and finally another contraction of the SWNT diameter (Figure 4ih). The change

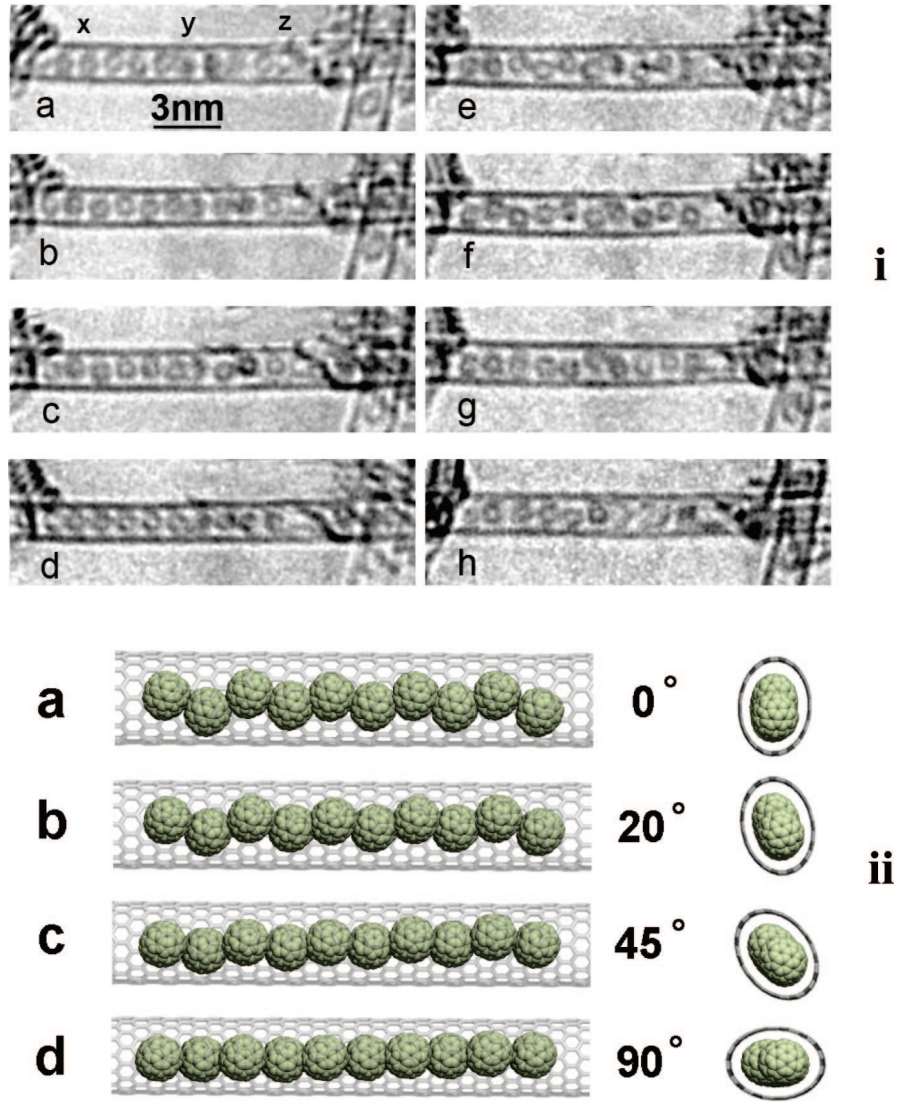

Figure 4. (i) TEM images of $Sc_3C_2@C_{80}$ SWNT peapods as a function of time. (a−h). Each image has 2 s acquisition and 10 s between frames. Three sections of the peapod are labeled as x, y, and z for future reference. (ii) Schematic representation of the rotation of a zigzag chain of $Sc_3C_2@C_{80}$ inside a SWNT causing structural deformation that leads to an elliptical cross section.

in diameter of the SWNT is driven by the rotation of the $Sc_3C_2@C_{80}$ chain with zigzag packing arrangement. The $Sc_3C_2@C_{80}$ adopt zigzag packing, which induces strain on the SWNT and causes the cross section of the SWNT to change from spherical to elliptical. Metal nanowires inside SWNTs can adopt static helical structures that produce similar distortions to the SWNT structure and lead to elliptical SWNT cross sections and diameter modulations.[33]

Figure 4ii shows a schematic representation of the $Sc_3C_2@C_{80}$ zigzag packing in a SWNT with an elliptical cross section at different rotation angles. The end on view is shown to the right in each case. In Figure 4iia, the fullerenes would appear in TEM as a zigzag chain with the largest interfullerene spacing and SWNT diameter. As the zigzag chain slowly rotates through to 90°, the diameter of the SWNT would appear to decrease in TEM, and the zigzag packing would appear as a 1D chain with a reduced interfullerene separation by 3−5%.

Damage to SWNTs by electron beam irradiation with energy above the damage threshold can lead to structural distortions and even to a change in diameter.[34] The van der Waals forces between carbon nanotubes in contact with other nanotubes or surfaces can also result in changes to the diameter of the carbon nanotubes.[35] Gloter et al. have observed a small increase in the diameter of a SWNT peapod and a change in the 1D packing of the fullerenes.[22] This observation is substantially different from ours in that the expansion was irreversible, it occurred for only a few fullerenes over a short distance, the energy of the electron beam was 120 kV and well above the damage threshold, and the peapod was in contact with another peapod giving rise to inter-SWNT van der Waals forces. In our observations, the reversible change in the SWNT diameter indicates it cannot be due to damage induced by the electron beam but must be caused by a reversible process. The low accelerating voltage of 80 kV used for the electron beam irradiation significantly reduces any structural damage to the peapod. The peapod is well isolated, and therefore van der Waals forces between touching peapods are negligible.

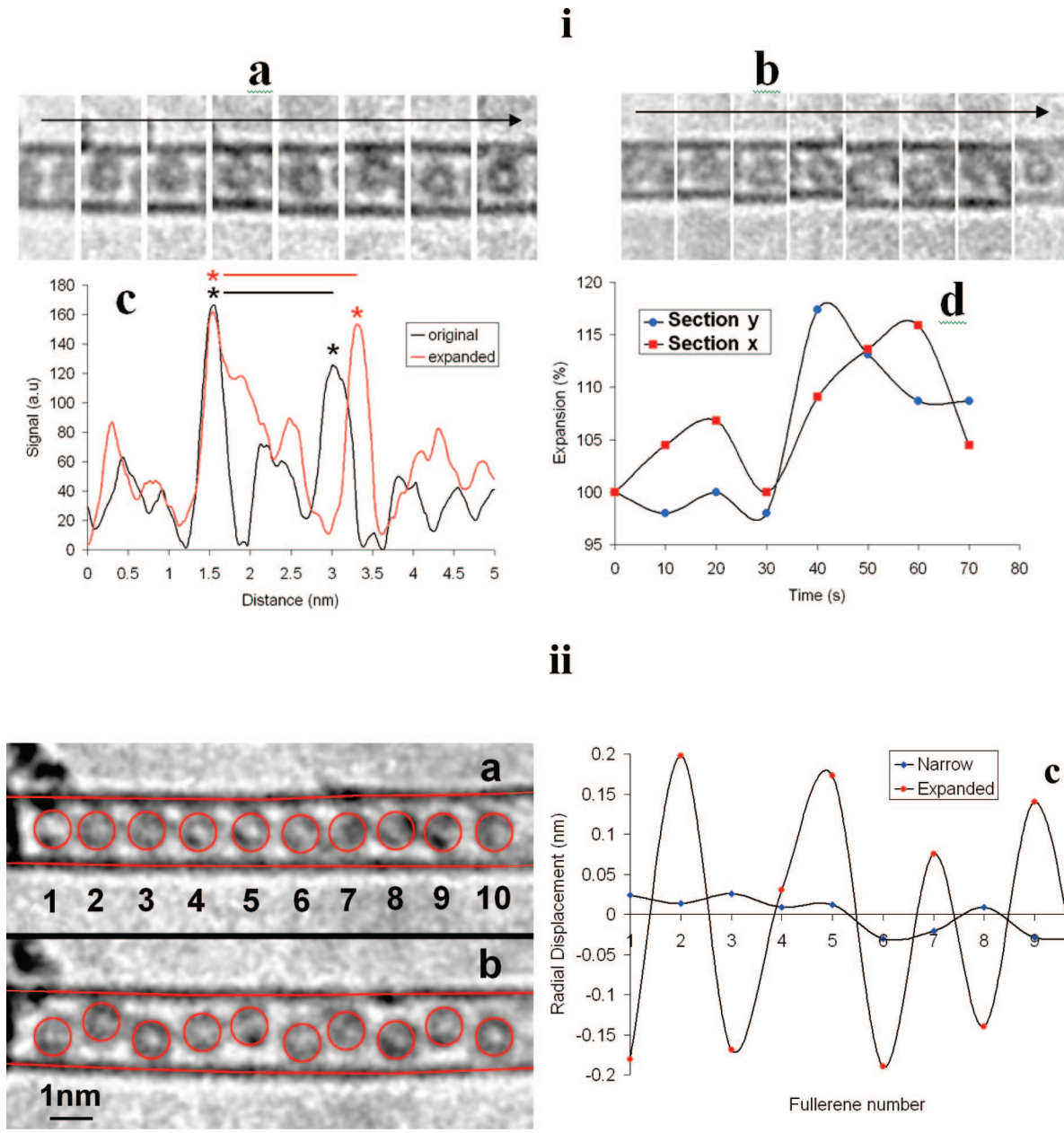

Figure 5. (i) (a) Time series of TEM images of section x of the $Sc_3C_2@C_{80}$ SWNT peapods, (b) time series of TEM images of section y of the $Sc_3C_2@C_{80}$ SWNT peapods, (c) line profile plot of intensity as a function of distance from the TEM image from section y showing the maximum expansion of the SWNT as compared with the original SWNT diameter (the peaks associated with the wall of the SWNT are indicated with an asterix), and (d) plot of the expansion of SWNT diameter as a function of time at both section x and section y. Expansion is measured from the line profile plots of TEM images as presented in Figure 5ic. (ii) TEM images used to measure the radial displacement of the (a) narrow SWNT and (b) expanded SWNT $Sc_3C_2@C_{80}$ peapods. (c) Plots the radial displacement of each $Sc_3C_2@C_{80}$ fullerene in the peapod for the respective images presented in parts a and b.

The change in the diameter of the SWNT is characterized in detail in Figure 5. The sections are labeled in the TEM image presented in Figure 5ia. Figure 5a presents a time series of TEM images of section x (front/left-hand side) of the peapod. The top of the SWNT sections have all been aligned in this image, and the changes in the diameter can be observed by monitoring the changes in the bottom of the SWNT section. As time progresses, the diameter of the SWNT is observed to expand and contract. Figure 5b presents the time series of TEM images from section y (middle) of the peapod. The diameter of the SWNT is also observed to expand and contract in this location as well. The behaviors of sections x and y of the peapod are not identical. To quantitatively analyze this expansion, a line profile from the TEM images is taken. The line profile plots the gray scale intensity as a function of distance across the peapod. The line profile for the middle section of the original and maximum expanded peapod is presented in Figure 5c. The peaks corresponding to the walls of the SWNT are marked with an asterisk. Using this method, we obtained precise measurements of the expansion of the peapod as a function of time for both section x and section y, shown in Figure 5d. From Figure 5d, the difference in the expansion behavior is apparent.

Section x expands for 20 s and then contracts for 10 s. This is followed by an expansion to both section x and section y in 10−20 s and a final contraction. The expansion reaches a maximum of 17% for section y after 40 s, while section x reaches a maximum expansion of 15.2% after 60 s. An expansion of 17% for the SWNT with a diameter of 1.5 nm corresponds to an increase of 0.26 nm.

In Figure 5ii, the radial displacement of the $Sc_3C_2@C_{80}$ metallofullerenes in the expanded peapod is compared with the case of the narrow contracted peapod. Red circles are overlaid on top of the metallofullerenes to give markers for the measurements. The distances from the center of the circle to both the bottom and the top walls of the SWNT were measured and used to determine the radial displacement. Figure 5iia shows a contracted peapod, in which the metallofullerenes are well-aligned with minimal deviation from the center region. Figure 5iib shows a maximum expanded peapod with the metallofullerenes displaced from the central region. Figure 5iic plots the radial displacement for each of the metallofullerenes in the peapod. A zigzag packing behavior is observed for the expanded peapod with a large increase in the degree of radial displacement as compared with the narrow contracted peapod. A maximum radial displacement of 0.2 nm was measured and this fits well with an expansion of 0.26 nm in the SWNT diameter. The average interfullerene distance also increased by 3.1% in going from the contracted peapod to the expanded peapod.

The observation of expansion in peapods may be favorable in $(Sc_3C_2)@C_{80}$ SWNT peapods due to the large charge transfer state of $(Sc_3{}^{9+}C_2{}^{3-})@C_{80}{}^{6-}$.[36] The larger number of electrons donated to the carbon cage should result in the energy of the highest occupied molecular orbit (HOMO) level being closer to the vacuum level and a smaller ionization potential than $Sc@C_{82}$, $La@C_{82}$, $Gd@C_{82}$, and C_{60}. This means that $Sc_3C_2@C_{80}$ should be easier to ionize under electron beam irradiation and produce charged fullerenes with large Coulomb repulsive forces in the peapods. One end of the $Sc_3C_2@C_{80}$ peapod is pinched off, and it is possible that somewhere along the peapod another constriction is present. In order to minimize Coulomb repulsive forces, charged metallofullerenes adopt zigzag packing and induce strain that causes the SWNT to expand in this radial direction. The zigzag chain of metallofullerenes slowly rotates inside the SWNT, and the diameter observed in TEM changes with time. By observing two successive expansion and contraction events, we have shown that a $Sc_3C_2@C_{80}$ metallofullerene peapod may potentially be used as a nanoactuator with subnanometer amplitude. For the realization of this novel phenomenon, it is important to drive the system with electrons of energy below the knock-on damage threshold and to have a filled peapod with at least one end sealed.

In summary, we have examined the time-dependent rotational dynamics of three different types of novel fullerene chains. Electrons with accelerating voltages of 80 kV induced coalescence of fullerenes in SWNT peapods without causing structural damage to the SWNTs. The resulting structures were then free to move within the SWNT host. The coalescence of C_{60} produced interesting asymmetric C_{300} fullerene structures that exhibited unique corkscrew rotation. C_{60} was also fused with $Sc@C_{82}$ and this structure also rotated while moving and also when stationary. The slow expansion and contraction of the diameter of the SWNT in $Sc_3C_2@C_{80}$ peapods due to the rotation of the zigzag fullerene chain is an exciting and entirely new phenomenon that has possibilities for nanoactuation. It may be that peapods could be integrated into nanodevices and driven using a noncontact method of electron beam irradiation to provide subnanometer mechanical control.

Acknowledgment. J.H.W. thanks the Sasakawa Fund for support. This research is part of the QIP IRC, www.qipirc.org, which is funded by EPSRC (GR/S82176/01). G.A.D.B. thanks EPSRC for a Professorial Research Fellowship (GR/S15808/01). H.S. is supported by the JSPS-CREST Program on Nanocarbons.

Supporting Information Available: TEM image, schematic representation, and measurement of C−C bond angles. This material is available free of charge via the Internet at http://pubs.acs.org.

References

(1) Avouris, P. Molecular electronics with carbon nanotubes. *Acc. Chem. Res.* **2002**, *35*, 1026.
(2) Kazaoui, S.; Minami, N.; Jacquemin, R.; Kataura, H.; Achiba, Y. *Phys. Rev. B* **1999**, *60*, 13339.
(3) Takenobu, T.; Takano, T.; Shiraishi, M.; Murakami, Y.; Ata, M.; Kataura, H.; Achiba, Y.; Iwasa, Y. *Nat. Mater.* **2003**, *2*, 683.
(4) Shimada, T.; Ohno, Y.; Okazaki, T.; Sugai, T.; Suenaga, K.; Kishimoto, S.; Mizutani, T.; Inoue, T.; Taniguchi, R.; Fukui, N.; Okubo, H.; Shinohara, H. *Physica E* **2004**, *21*, 1089.
(5) Shimada, T.; Okazaki, T.; Taniguchi, R.; Sugai, T.; Shinohara, H.; Suenaga, K.; Ohno, Y.; Mizuno, S.; Kishimoto, S.; Mizutani, T. *Appl. Phys. Lett.* **2002**, *81*, 4067.
(6) Jaroenapibal, P.; Chikkannanavar, S. B.; Luzzi, D. E.; Evoy, S. *J. Appl. Phys.* **2005**, *98*, 044301.
(7) Khlobystov, A. N.; Britz, D.; Ardavan, A.; Briggs, G. A. D. *Phys. Rev. Lett.* **2004**, *92*, 245507.
(8) Khlobystov, A. N.; Scipioni, R.; Nguyen-Manh, D.; Britz, D.; Pettifor, D. G.; Briggs, G. A. D.; Lyapin, S. G.; Ardavan, A.; Nicholas, R. J. *Appl. Phys. Lett.* **2004**, *84*, 792.
(9) Hirahara, K.; Bandow, S.; Suenaga, K.; Kato, H.; Okazaki, T.; Shinohara, H.; Iijima, S. *Phys. Rev. B* **2001**, *64*, 115420.
(10) Suenaga, K.; Okazaki, T.; Hirahara, K.; Bandow, S.; Kato, H.; Taninaka, A.; Shinohara, H.; Iijima, S. *Appl. Phys. A: Mater. Sci. Process.* **2003**, *76*, 445.
(11) Smith, B. W.; Luzzi, D. E.; Achiba, Y. *Chem. Phys. Lett.* **2000**, *331*, 137.
(12) Hirahara, K.; Suenaga, K.; Bandow, S.; Kato, H.; Okazaki, T.; Shinohara, H.; Iijima, S. *Phys. Rev. Lett.* **2000**, *85*, 5384.
(13) Suenaga, K.; Okazaki, T.; Wang, C.-R.; Bandow, S.; Shinohara, H.; Iijima, S. *Phys. Rev. Lett.* **2003**, *90*, 055506.
(14) Khlobystov, A. N.; Porfyrakis, K.; Kanai, M.; Britz, D. A.; Ardavan, A.; Shinohara, H.; Dennis, T. J. S.; Briggs, G. A. D. *Angew. Chem., Int. Ed.* **2004**, *43*, 1386.
(15) Yoon, M.; Berber, S.; Tomanek, D. *Phys. Rev. B* **2005**, *71*, 155406.
(16) Britz, D. A.; Khlobystov, A. N.; Porfyrakis, K.; Ardavan, A.; Briggs, G. A. D. *Chem. Commun.* **2005**, 37.
(17) Koshino, M.; Tanaka, T.; Solin, N.; Suenaga, K.; Isobe, H.; Nakamura, E. *Science* **2007**, *316*, 853.
(18) Liu, Z.; Koshino, M.; Suenaga, K.; Mrzel, A.; Kataura, H.; Iijima, S. *Phys. Rev. Lett.* **2006**, *96*, 088304.
(19) Liu, Z.; Yangai, K.; Suenaga, K.; Kataura, H.; Iijima, S. *Nat. Nanotech.* **2007**, *2*, 422.
(20) Krasheninnikov, A. V.; Banhart, F. *Nat. Mater.* **2007**, *6*, 723.
(21) Hernandez, E.; Meunier, V.; Smith, B. W.; Rurali, R.; Terrones, H.; Buongiorno Nardelli, M.; Terrones, M.; Luzzi, D. E.; Charlier, J.-C. *Nano Lett.* **2003**, *3*, 1037.

(22) Gloter, A.; Suenaga, K.; Kataura, H.; Fujii, R.; Kodama, T.; Nishikawa, H.; Ikemoto, I.; Kikuchi, K.; Suzuki, S.; Achiba, Y.; Iijima, S. *Chem. Phys. Lett.* **2004**, *390*, 462.
(23) Urita, K.; Sato, Y.; Suenaga, K.; Gloter, A.; Hashimoto, A.; Ishida, M.; Shimada, T.; Shinohara, H.; Iijima, S. *Nano Lett.* **2004**, *4*, 2451.
(24) Li, J.; Banhart, F. *Nano Lett.* **2004**, *4*, 1143.
(25) Vijayaraghavan, A.; Kanzaki, K.; Suzuki, S.; Kobayashi, Y.; Inokawa, H.; Ono, Y.; Kar, S.; Ajayan, P. M. *Nano Lett.* **2005**, *5*, 1575.
(26) Banhart, F.; Ajayan, P. M. *Nature* **1996**, *382*, 433.
(27) Krasheninnikov, A. V.; Banhart, F. *Nat. Mater.* **2007**, *6*, 723.
(28) Hernandez, E.; Meunier, V.; Smith, B. W.; Rurali, R.; Terrones, H.; Buongiorno Nardelli, M.; Terrones, M.; Luzzi, D. E.; Charlier, J.-C. *Nano Lett.* **2003**, *3*, 1037.
(29) Warner, J. H.; Watt, A. A. R.; Ge, L.; Porfyrakis, K.; Akachi, T.; Okimoto, H.; Ito, Y.; Ardavan, A.; Montanari, B.; Jefferson, J. H.; Harrison, N. M.; Shinohara, H.; Briggs, G. A. D. *Nano Lett.* **2008**, *8*, 1005.
(30) Shinohara, H. *Rep. Prog. Phys.* **2000**, *63*, 843.
(31) Niyogi, S.; Hamon, M. A.; Hu, H.; Zhao, B.; Bhowmik, P.; Sen, R.; Itkis, M. E.; Haddon, R. C. *Acc. Chem. Res.* **2002**, *35*, 1105.
(32) Haddon, R. C. *Science* **1993**, *261*, 1545.
(33) Philp, E.; Sloan, J.; Kirkland, A. I.; Meyer, R. R.; Friedrichs, S.; Hutchinson, J. L.; Green, M. L. H. *Nat. Mater.* **2003**, *2*, 788.
(34) Smith, B. W.; Luzzi, D. E. *J. Appl. Phys.* **2001**, *90*, 3509.
(35) Hertel, T.; Walkup, R. E.; Avouris, P. *Phys. Rev. B* **1998**, *58*, 13870.
(36) Tan, K.; Lu, X. *J. Phys. Chem. A* **2006**, *110*, 1171.

NL801149Z